J. Fluid Mech. (1978), *vol.* 84, *part* 4, *pp.* 641–656
Printed in Great Britain

Similarity in the initial region of annular jets: three configurations

By N. W. M. KO AND W. T. CHAN
Department of Mechanical Engineering, University of Hong Kong

(Received 12 May 1977)

This paper describes part of a detailed study of the initial region of three annular jets. The configurations are the basic one, without any bullet in the centre, and those with a conical and an elliptical bullet. From the mean velocity and turbulence intensity measurements the initial region can be divided into the initial merging, the intermediate and the fully merged zones. Within these three zones similarity of both the mean velocity and the turbulence intensity profiles has been found. The similarity curves are compared with those for a single jet.

1. Introduction

The initial region of an annular air jet discharging into stationary air has been only scantily investigated. The early work of Miller & Comings (1960) concerned the flow structure of dual plane jets issuing into stationary air. Their measurements showed the subatmospheric pressure region due to entrainment in the centre. This region was also responsible for the convergence of the dual jets towards the central axis. Associated with the subatmospheric pressure region was the recirculating vortex which recycled air in this region. The measurements of an annular jet by Chigier & Beer (1964) were part of an investigation into the flow structure of coaxial or concentric jets. Their mean velocity and static pressure measurements also established the presence of a subatmospheric region and a vortex in the centre of the annular jet.

The recent investigation of Ayukawa & Shakouchi (1976) involved a two-dimensional jet attaching to a wall, which also formed a subatmospheric pressure region and the associated vortex. The work mainly concerned the periodic pressure fluctuations within the subatmospheric pressure region.

Though the above-mentioned work included mean velocity and turbulence intensity measurements, an investigation of similarity of these profiles has not been attempted. In this respect, the purpose of the present investigation was to obtain information about the flow characteristics within the initial region of three annular jets: a basic annular jet, a conical jet and an ellipsoidal jet. This paper presents the first part of the investigation, which concerns the mean velocity, turbulence intensity and their similarity. The latter parts will concern the spectral and correlation measurements of both the turbulence and the pressure fluctuations, which are associated with the recirculating vortex in the centre and the vortices in the outer mixing region.

From the similarity curves of the mean velocity and turbulence intensity, the initial region of the annular jets can be separated into the initial merging, the

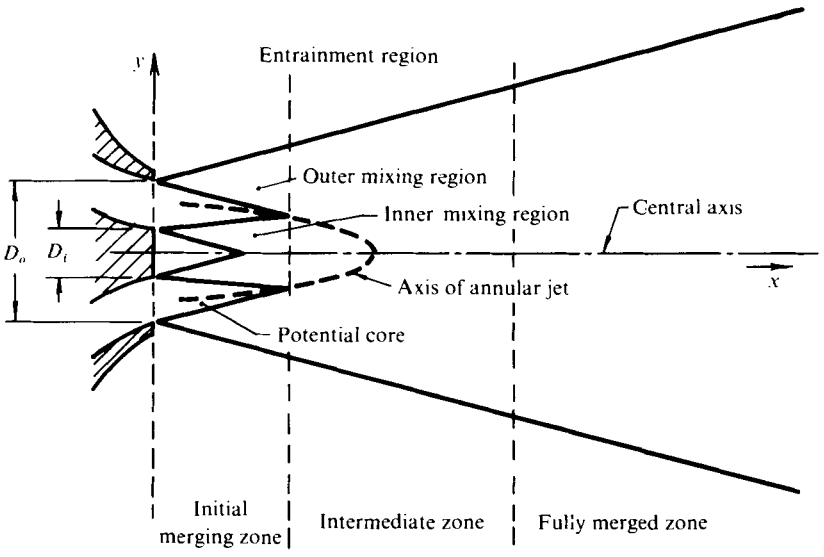

FIGURE 1. Schematic profile of initial region of annular jet.

intermediate and the fully merged zones. An attempt will be made to compare the similarity curves obtained from this investigation with the available results for a single jet.

2. Apparatus

The experiments were carried out within annular jets of three configurations. A diagram of the arrangement of the nozzles of the three configurations is shown in figure 1. Basically, at the nozzle exit the circular annular nozzle has an outer diameter D_0 of 6·2 cm and an inner diameter D_i of 2·8 cm. The area contraction ratio of the nozzles was 15:1. The first configuration was the basic 'annular' nozzle, without any protrusion or bullet at the nozzle exit. With this type of configuration an internal recirculating vortex of toroidal form was found (Chigier & Beer 1964). The other two configurations included a bullet-like protrusion. The intention was to eliminate the internal recirulating vortex found in the basic annular configuration. At the exit the diameter of the bullet was the same as the inner diameter D_i of the annular jet so that no discontinuity of flow occurred. The profile of the bullet in the second configuration was 'conical', while in the third it was 'ellipsoidal'. The length of both the conical and the ellipsoidal bullet was 1·5 D_0. This length was adopted so that the internal recirculating vortex was estimated. For simplification the jet with the basic configuration is simply termed an 'annular' jet while the other two are termed 'conical' and 'ellipsoidal'.

The nozzle was supplied with dry, oil-free, high-pressure air from an air reservoir. The nozzle has a Burgess-type silencer as its settling chamber. The noise from the upstream control valve was mostly absorbed by a resonator-type silencer before it arrived at the nozzle exit. Further absorption of the inherent noise was achieved by passing the air from the silencer through a layer of 2 mm polyurethane material. In this way, besides having a lower inherited background level, the flow was smoothed,

resulting in a lower local turbulence intensity at the exit. In the velocity range of this investigation the inherited overall background pressure level at the exit was 99 dB. The background turbulence intensity level was 0·22 % of the mean exit velocity. The inclusion of the conical or ellipsoidal bullet did not significantly affect the background conditions at the exit.

The hot-wire anemometer used was of constant-temperature type with a linearized output (Davies & Davies 1966). Only a single wire was used in the present work. This wire, consisting of tungsten, had a diameter of 5×10^{-6} m and a length of 2 mm. Its operating resistance was about 15 Ω.

The domain of investigation was mostly confined to the first seven outer diameters D_0 downstream of the nozzle exit. However, the small dimensions of and the complicated flow pattern in the inner mixing region made it difficult to investigate this region accurately. Thus the main effort was expended on the outer mixing region. Nevertheless, limited measurements have been obtained in the inner mixing region. Because of the difficulty encountered in this mixing region, no attempt was made to correct the single-wire results for the deviation in the flow direction from axial. The mean exit velocity in the investigation was 50 ms^{-1}. Though another set of measurements, for an exit velocity of 30 ms^{-1}, has also been obtained for comparison, it will not be presented.

3. Mean velocity

Domain

The mean velocity profiles for an annular jet have been obtained by Chigier & Beer (1964). They simply separated the annular jet into the merging zone and the combined jet. This division did not fully describe the flow structures in the initial region. Thus a division similar to that for coaxial jets (Kwan & Ko 1976) is adopted. The annular jets are divided into the initial merging zone, the intermediate zone and the fully merged zone (figure 1). The zone which is nearest to the nozzle exit and ends roughly at the plane where the potential core disappears is called the initial merging zone. It is within this zone that the internal recirculating vortex is found in the annular potential core for the annular jet and the bullet is found for the conical and ellipsoidal jet. As in the case of single and coaxial jets, the mean velocity within the annular potential core is the same as the jet exit velocity $\overline{U}_0$.

Immediately downstream of the initial merging zone is the intermediate zone. It is within this zone that mixing of the flows from the annular potential core and from the outer mixing region occurs. It is also within the intermediate zone that the axis of the annular potential core and the high mean velocity associated with the potential core merge at the central axis of the nozzle. The extent of this intermediate zone, as will be discussed later, is about three outer diameters D_0.

The fully merged zone is the one downstream of the intermediate zone. Within this zone complete merging of the flows from the initial merging zone has occurred. The fully merged flow behaves like a combined jet and its characteristics are similar to those of a single jet.

Though the above delineation of the three zones is approximate, it will be supported by good similarity of the mean velocity and turbulence intensity profiles observed in these zones.

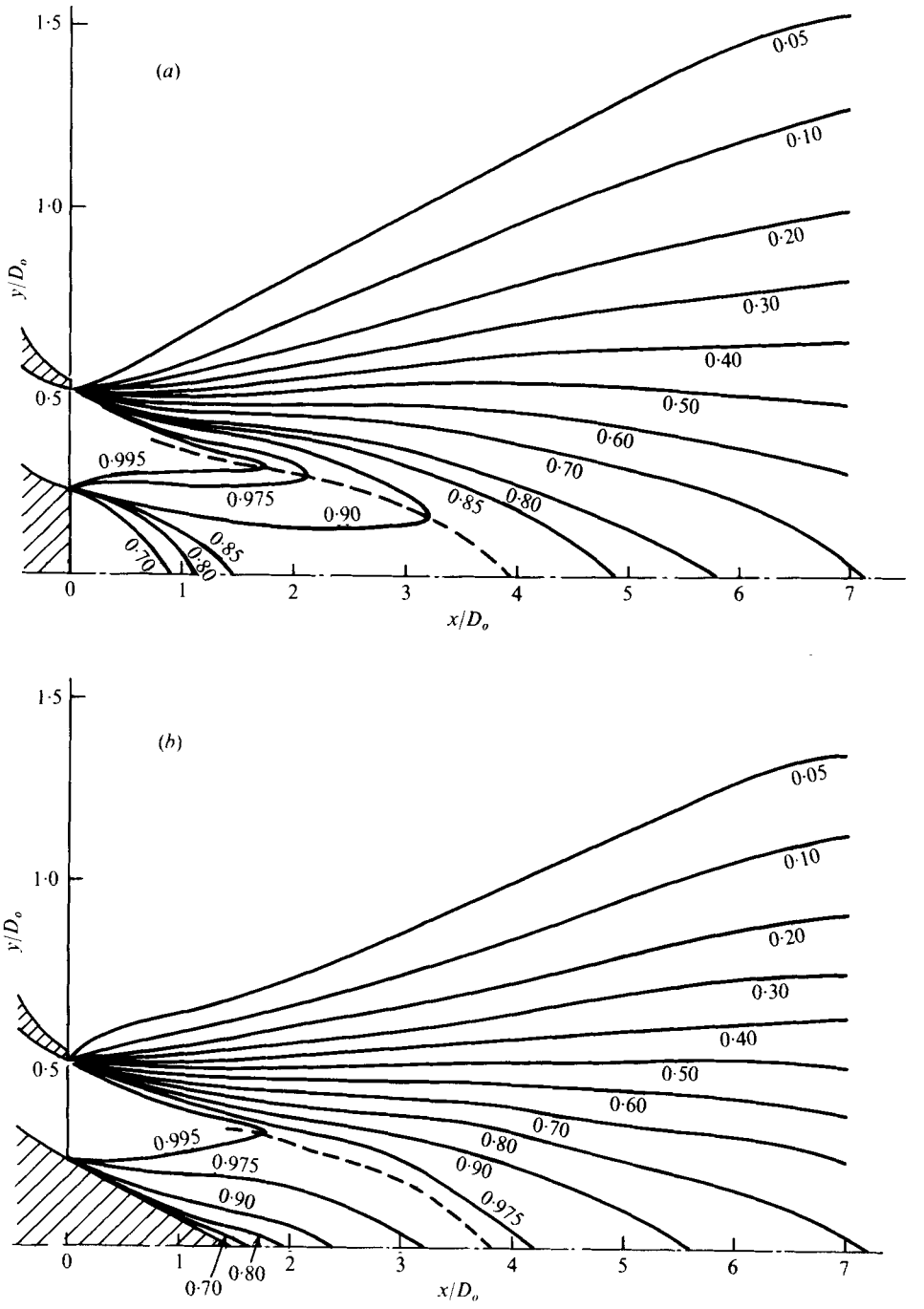

FIGURES 2 (*a*, *b*). For legend see next page.

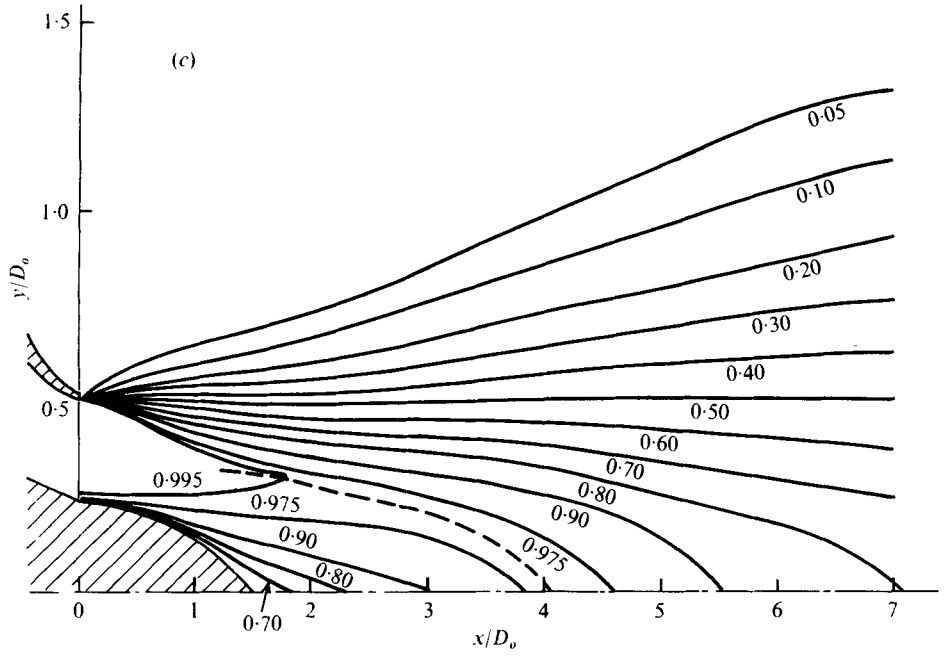

FIGURE 2. Mean velocity contours. (*a*) Annular jet. (*b*) Conical jet. (*c*) Ellipsoidal jet.

Mean velocity contours

The contours of the local mean velocity ratio $\overline{U}/\overline{U}_0$ of the annular, conical and ellipsoidal jets are shown in figures 2(*a*), (*b*) and (*c*) respectively. As shown in figure 2(*a*), the entrainment in the central region of the annular jet is responsible for the generation of the internal recirculating vortex of toroidal form (Chigier & Beer 1964). This recirculating vortex is mainly found within the first half-diameter downstream of the nozzle exit. Because of this vortex, the associated subatmospheric pressure and the radial pressure forces draw the potential core towards the central axis. Besides the above displacement, figure 2(*a*) also shows that the contours corresponding to mean velocity ratios $\overline{U}/\overline{U}_0 \geqslant 0{\cdot}6$ are also displaced towards the central axis. The contour $\overline{U}/\overline{U}_0 = 0{\cdot}5$, however, is roughly parallel to the central axis and is not really affected by the subatmospheric region associated with the vortex. For the contours with $\overline{U}/\overline{U}_0 \leqslant 0{\cdot}4$ outward displacement is found and is mainly influenced by the entrainment region outside.

Like the results for the annular jet, the contours for $\overline{U}/\overline{U}_0 \leqslant 0{\cdot}5$ for the conical and ellipsoidal jets, as shown in figures 2(*b*) and (*c*), are mainly influenced by the outer entrainment region. Similarly, the effect of the inner entrainment is felt for $\overline{U}/\overline{U}_0 \geqslant 0{\cdot}6$, in spite of the presence of the bullets.

Comparison of the mean velocity contours for the conical and ellipsoidal jets shows that the contours for $\overline{U}/\overline{U}_0 \leqslant 0{\cdot}5$ are basically identical and have the same angle of spread. Even though the vortex in the centre is eliminated by the bullet, a certain amount of entrainment is still present, resulting in the displacement of the annular potential core towards the central axis. However, no appreciable difference in the contours for $0{\cdot}80 \geqslant \overline{U}/\overline{U}_0 \geqslant 0{\cdot}6$ is found. The noticeable difference between the two

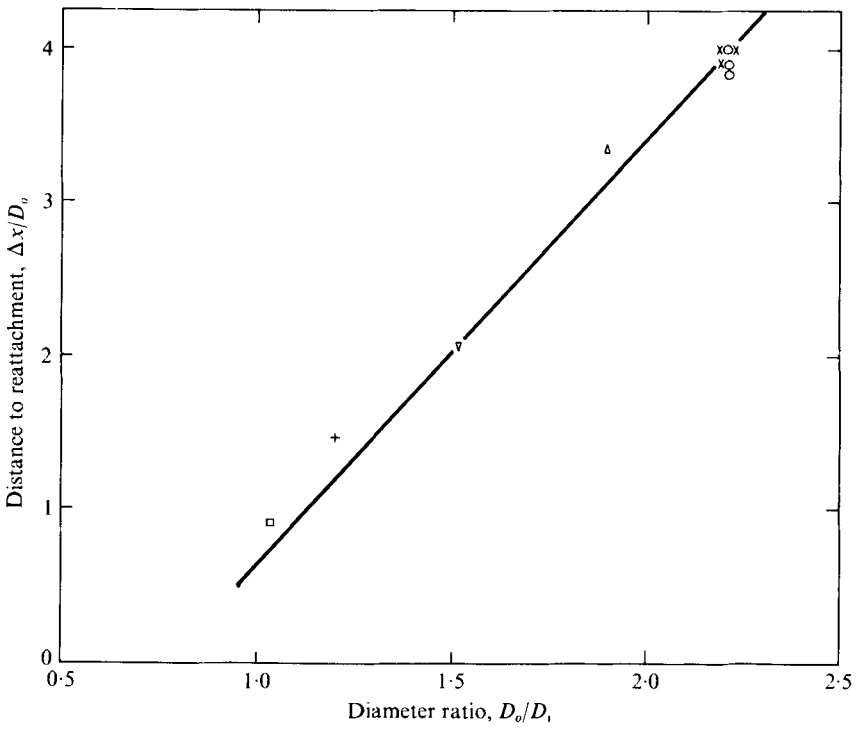

FIGURE 3. Variation of reattachment position with diameter ratio. ○, 50 ms^{-1}; ×, 30 ms^{-1}; △, 50 ms^{-1}; ▽, Chigier & Beer; +, Miller & Comings; □, Ayukawa & Shakouchi.

jets is in the contours for $\overline{U}/\overline{U}_0 \geqslant 0{\cdot}90$. This is due to the shapes of the two bullets used: the conical bullet results in slightly higher degree of entrainment than the ellipsoidal one. This may be the reason for the bigger displacement of the contours towards the central axis for the conical jet than for the ellipsoidal jet.

Comparison between the annular jet and the other two jets shows that, although the contours $\overline{U}/\overline{U}_0 = 0{\cdot}50$ of all the jets are at the radial position $y/D_o = 0{\cdot}5$, the spread of the outer mixing region of the annular jet (figure 2*a*) is slightly bigger than that of the other two. As would be expected, the contours with $\overline{U}/\overline{U}_0 \geqslant 0{\cdot}60$ of the annular jet are displaced more towards the central axis. It is due to the presence of the subatmospheric pressure region in the centre.

Also from figure 2, the position at which the annular potential core ($\overline{U}/\overline{U}_0 = 0{\cdot}995$) of the three jets ends is found at $x/D_o \simeq 1{\cdot}7$, $y/D_o \simeq 0{\cdot}3$. It is independent of the conditions in the centre of the jet. Even though the termination position is the same, the shape of the potential core is affected by the conditions in the centre. This leads one to expect the shape of the potential core of the annular jet to be noticeably smaller than that of the other two.

As for the potential core, figure 2 further indicates that the end of the axis of the annular jet (figure 1), or the point of reattachment, is also independent of the conditions inside the jet. For the three jets shown in figure 2 the axial position of reattachement is $x/D_o \simeq 4$. This means that, irrespective of the presence of either the internal vortex or the bullet, the high velocity flow which is inherited from the annular potential core merges at this axial position $x/D_o \simeq 4$.

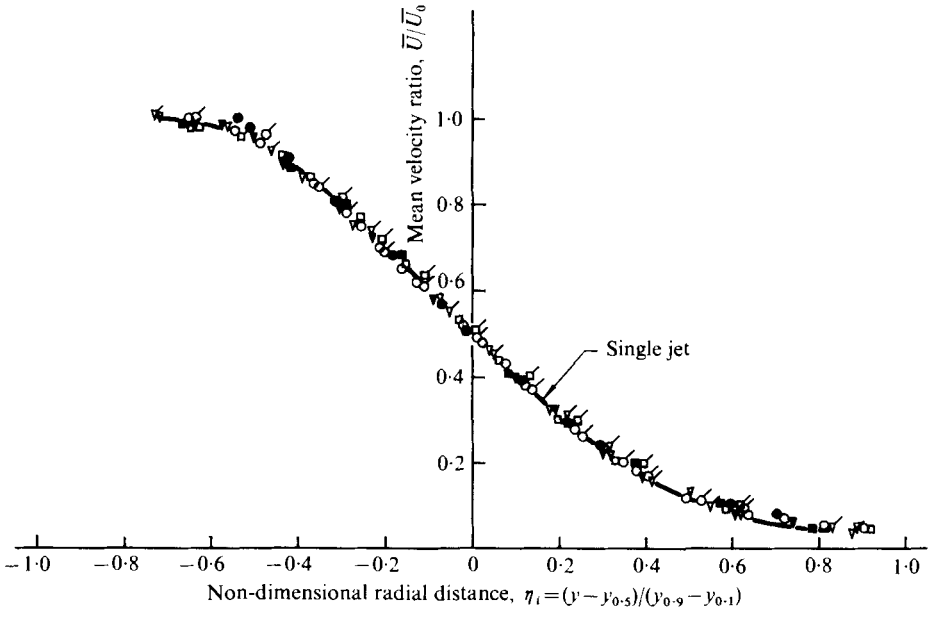

FIGURE 4. Similarity of mean velocity ratio in initial merging zone. Annular, x/D_o: ○, 0·5; △, 0·75; ▽, 1·0; □, 2·0. Conical, x/D_o: ●, 0·5; ▲, 0·75; ▼, 1·0; ◀, 1·5; ■, 2·0. Ellipsoidal, x/D_o: ◇, 0·5; ◈, 1·0; ◁, 1·5; ▱, 1·75; ◫, 2·0.

This axial position $x/D_o \simeq 4$ for reattachment has also been observed at the lower exit velocity of 30 ms^{-1}. In other words, the exit velocity does not affect this position.

The position of reattachement of an annular jet has also been given by Chigier & Beer (1964). At a jet exit velocity of 36 ms^{-1} reattachment was found at an axial position of 2·06 D_o. The corresponding position for two-dimensional dual jets with an exit velocity of 22 ms^{-1} was found at 1·47 D_o by Miller & Comings (1960). For the two-dimensional jet attaching to a wall of Ayukawa & Shakouchi (1976) the axial position of reattachment was 0·94 D_o, for an exit velocity of 30 ms^{-1}. In the results of Miller & Comings (1960) and Ayukawa & Shakouchi (1976) slight extrapolation was adopted to obtain the merging distance at the central axis.

Together with the annular-jet results obtained with the nozzle configuration of Ko & Kwan (1976), the reattachment distance is correlated and plotted in figure 3. Extremely good correlation is found with the nozzle diameter ratio D_o/D_i. This good correlation is interesting because the results of Miller & Comings (1960) and Ayukawa & Shakouchi (1976) are for two-dimensional jets. Further, the latter work was for a jet attaching to a wall.

The trend of the reattachment distance with the diameter ratio D_o/D_i shown in figure 3 suggests that for bigger diameter ratios reattachment occurs further downstream. This phenomenon may be due to the larger momentum associated with a jet of bigger diameter ratio. This reasoning is supported by the work of Miller & Comings (1960) and later of Chigier & Beer (1964), which stated that the total momentum flux was conserved. In the case of the initial region of the annular jet the momentum due to the fluctuating axial velocity was small compared with that due to the mean axial velocity and that due to the mean static pressure. Chigier & Beer (1964) have further

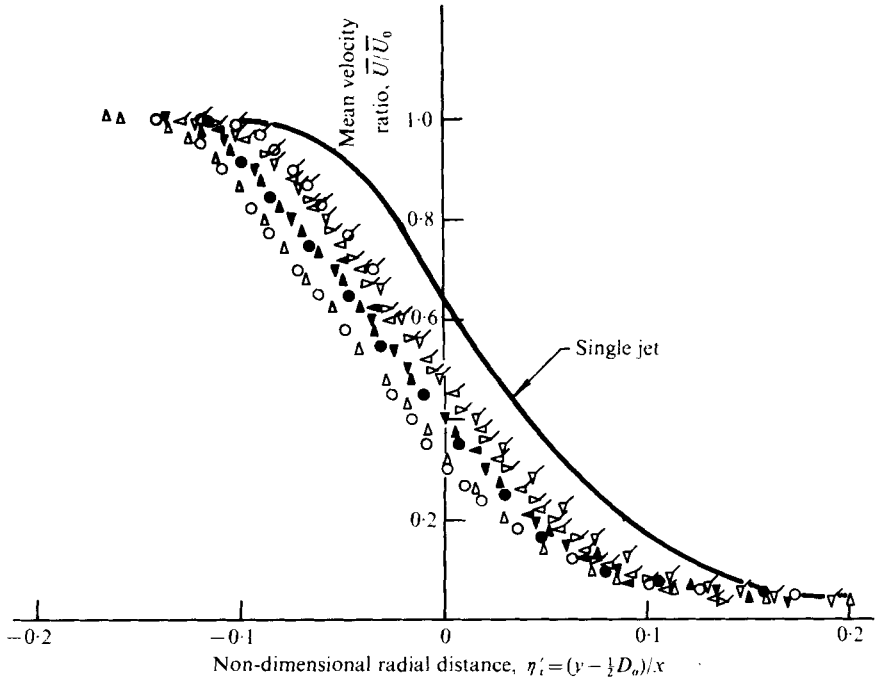

FIGURE 5. Similarity of mean velocity ratio in initial merging zone. Symbols same as in figure 4.

observed that the pressure term was not as dominant as the mean velocity term. It was estimated that the pressure term reached a maximum value of 15% of the total input momentum. According to this, the higher input momentum associated with the higher D_o/D_i would result in a mean velocity momentum flux higher than that due to the pressure. On balance, this higher mean velocity momentum would be responsible for the shift of the reattachment further downstream.

Similarity

Similarity of the local mean velocity profiles in the different zones of the three jets is discussed in this subsection. For the initial merging zone the similarity curves for the outer mixing region of the annular, conical and ellipsoidal jets are shown in figure 4. In this figure the non-dimensional mean velocity ratio $\bar{U}/\bar{U}_0$ is plotted against the non-dimensional radial distance $\eta_i = (y - y_{0.5})/(y_{0.9} - y_{0.1})$, where $y_{0.9}$, $y_{0.5}$ and $y_{0.1}$ are the radial positions where the local mean velocity is equal to 0·9, 0·5 and 0·1 of the jet exit velocity $\bar{U}_0$. This non-dimensional radial distance was suggested by Abramovich (1963, p. 9) for coaxial-jet results. For their coaxial-jet results Ko & Kwan (1976) also found that η_i was a better non-dimensional radial distance for the primary mixing region than $(y - \frac{1}{2}D_i)/x$.

Using the non-dimensional distance η_i, very good similarity of the local mean velocity profiles for axial distances $0{\cdot}5 \leqslant x/D_o \leqslant 2$ is found for all three jets (figure 4). For $x/D_o = 3$ only slight deviation from the similarity curve is found. Further than three outer diameters downstream progressively greater deviation is observed. The single-jet result is also shown in figure 4. Very good agreement of the

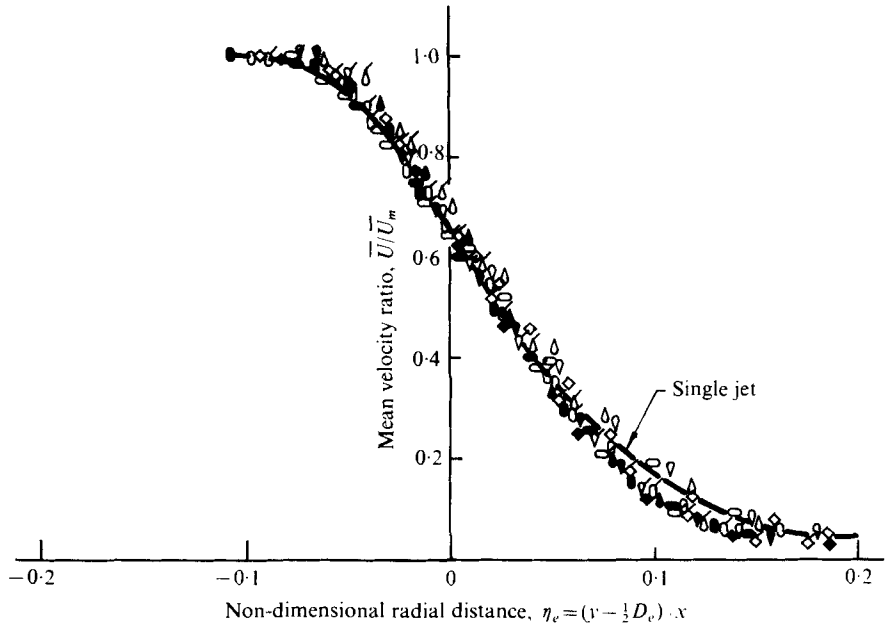

FIGURE 6. Similarity of mean velocity ratio in intermediate and fully merged zone. Annular, x/D_o: ◇, 3; ▯, 4; ⬭, 5; ▽, 6; ◇, 7. Conical, x/D_o: ◆, 3; ▮, 4; ⬬, 5; ▼, 6; ▲, 7. Ellipsoidal, x/D_o: ◇, 3; ▱, 4; ▱, 5; ▽, 6; ▱, 7.

similarity curve for the single jet with those for the three jets of this investigation is found.

Besides the correlation with the non-dimensional radial distance η_i, similarity of the mean velocity profiles in the outer mixing region with $\eta_i' = (y - \frac{1}{2}D_o)/x$ has also been investigated. This non-dimensional radial distance was suggested for the single jet by Davies, Fisher & Barratt (1963) and other workers. Within the same range of axial distances $0{\cdot}5 \leqslant x/D_o \leqslant 2$, very good similarity is found for the velocity profiles of each jet measured here (figure 5). However, when a comparison is made with the single jet, differences are found.

The greatest deviation of the similarity curve from that for a single jet is found for the annular jet. The curve is displaced further towards the central axis. For the conical jet, however, less displacement towards the central axis is found while the displacement for the ellipsoidal jet is the least of the three. This difference in the deviations of the similarity curve within the initial merging zone illustrates clearly the effect of the entrainment in the centre on the mean velocity. As would be expected, the presence of the subatmospheric static pressure region and the presence of the two different bullets in the centre cause the difference in the deviation.

In the intermediate and fully merged zone similarity of the mean velocity ratio $\overline{U}/\overline{U}_m$ with the non-dimensional distance $\eta_e = (y - \frac{1}{2}D_e)/x$ is found (figure 6), $\overline{U}_m$ being the maximum mean velocity in the x, y plane and D_e the equivalent diameter of the fully merged jet. The equivalent jet is derived from the idea of Eldred *et al.* (1971) that the fully merged jet can be represented by an equivalent jet of identical thrust having a diameter D_e and an equivalent exit velocity $\overline{U}_e$. In the present case $\overline{U}_e$ is equal to $\overline{U}_m$.

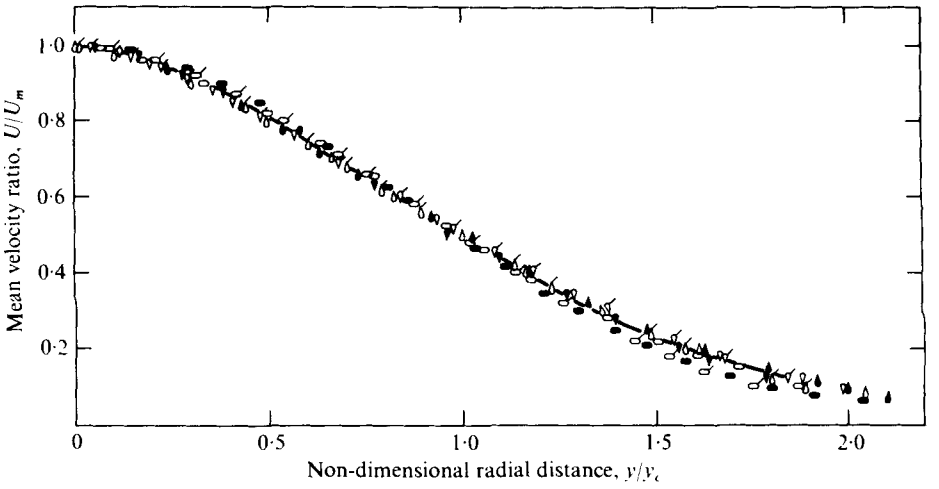

FIGURE 7. Similarity of mean velocity ratio in fully merged zone. Symbols same as in figure 6.

As shown by figure 6, good similarity of the three jets over axial distances $3 \leqslant x/D_o \leqslant 7$ has been found. In addition, good agreement with the single-jet results has been found. However, more detailed comparison in figure 6 shows better agreement for $\eta_e \leqslant 0$ and slight deviation from the single-jet results for $\eta_e \geqslant 0$. For $\eta_e \geqslant 0$ the results for the annular jet agree slightly better than those for the conical and ellipsoidal jets.

Though similarity based on η_e has been shown to be good, in the fully merged zone the similarity of $\bar{U}/\bar{U}_m$ with the non-dimensional radial distance y/y_c has been found to be better in all three jets (figure 7). Here y_c is the radial distance at which the local mean velocity is equal to 0·5 of $\bar{U}_m$. This better similarity is observed only for $x/D_o \geqslant 5$. Furthermore, very good agreement with the single-jet results in the fully developed region has also been found.

This good similarity in the fully merged zone suggests that all three jets are self-preserving from an axial distance of five outer diameters downstream of the nozzle exit. The good agreement with the single-jet results in the same region suggests that the combined jets behave exactly like a single jet.

The results discussed above were for an exit velocity of 50 ms^{-1}. Results for an exit velocity of 30 ms^{-1}, not shown in this paper, have also been obtained. Detailed comparison between the two sets of results indicates the same similarity of the mean velocity ratios in the initial merging zone, the intermediate zone and the fully merged zone. Because the similarity is the same, good agreement with the single-jet results is found. This independence of the similarity of the exit velocity is the same phenomenon as is observed in single jets (Davies *et al.* 1963; and others).

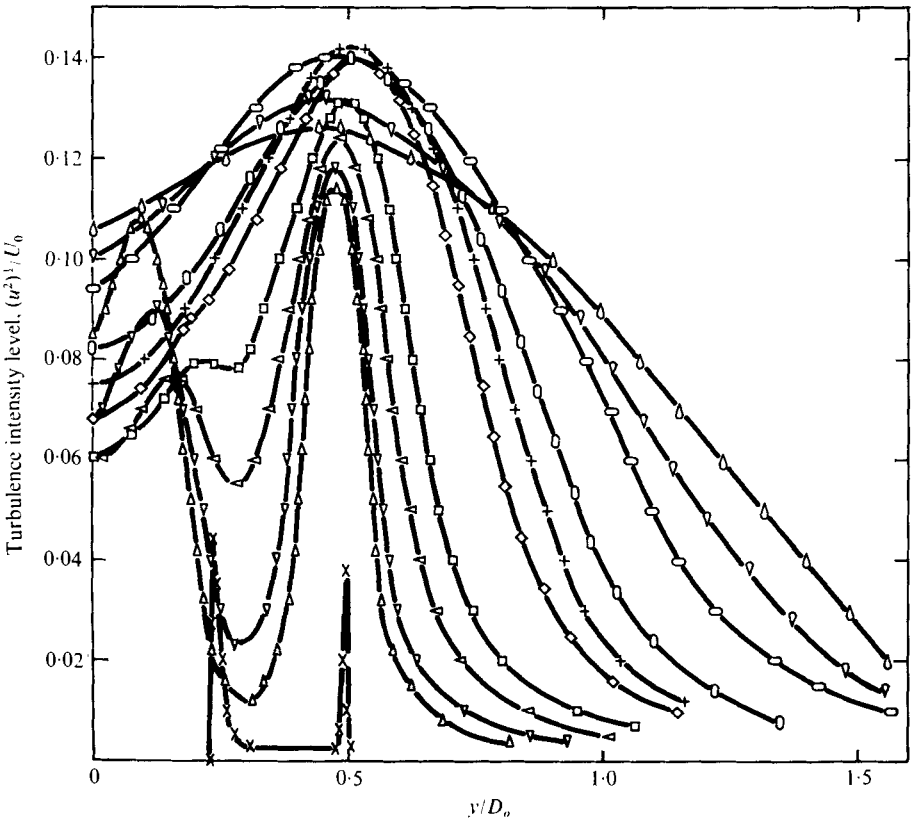

FIGURE 8. Distribution of turbulence intensity level of annular jet. x/D_o: ×, 0; ◁, 1·5; +, 3·5. Other symbols same as in figures 4 and 6.

4. Turbulence intensity

Distribution

The axial distribution of the turbulence intensity profiles of the annular jet is shown in figure 8. Because the profiles of the conical and ellipsoidal jets are basically the same, except in the inner mixing region, they are not shown in the present paper. Fundamentally, within the outer mixing region one peak in the turbulence intensity profiles is found for all three jets. Over the whole axial distance considered, $0 \leqslant x/D_o \leqslant 7$, the peak in the outer mixing region is located at the radial position $y/D_o \simeq 0{\cdot}5$. This radial position of the peak is roughly the same as that for a single jet (Davies *et al.* 1963; Mollo-Christensen, Kolpin & Martuccelli 1964; and others). However, as will be discussed later, there is a slight displacement of the radial position of the peak turbulence intensity towards the central axis.

The position of the peak turbulence intensity in the inner mixing region of the annular jet is different from those for the conical and ellipsoidal jets. For the annular jet the peak becomes displaced away from the central axis as the axial distance is increased. At the axial position $x/D_o \simeq 3$, i.e. in the intermediate zone, the peak turbulence intensity is masked by the intensity level of the outer mixing region.

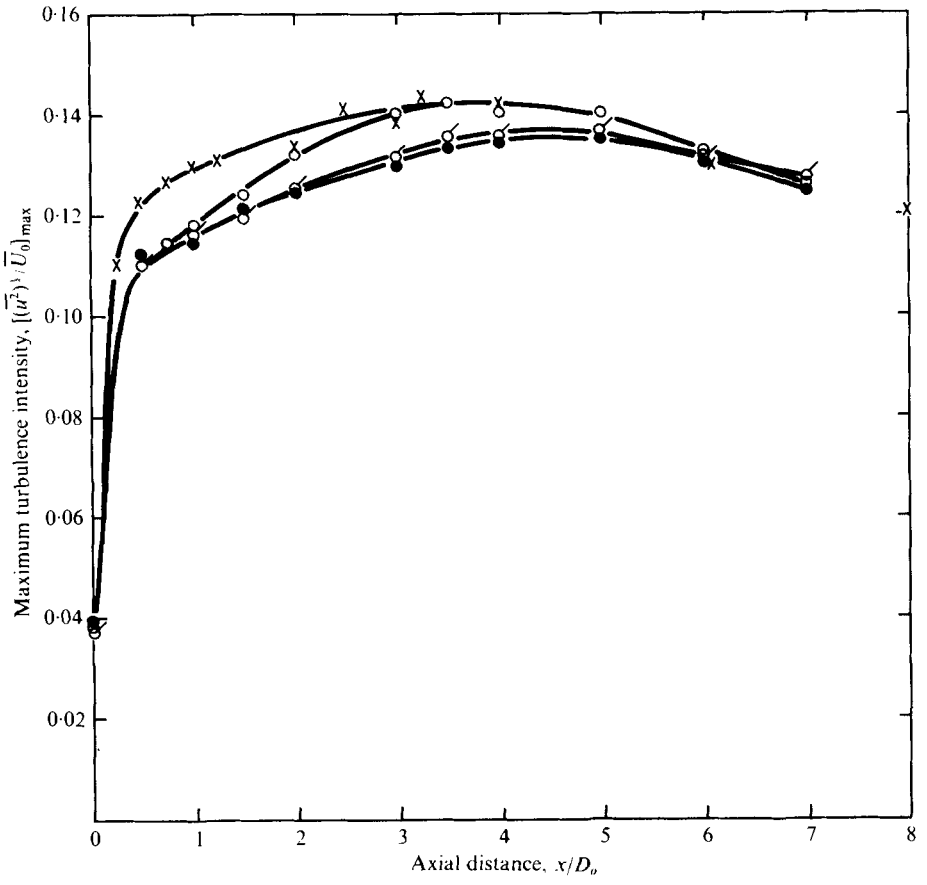

FIGURE 9. Axial distribution of maximum turbulence intensity level. ○, annular jet; ●, conical jet; ♂, ellipsoidal jet; ×, single jet.

For the conical and ellipsoidal jets the peak intensity tends to shift towards the central axis at larger distances downstream. The axial position where the peak turbulence of the inner mixing region is masked by the local turbulence of the outer mixing region is at $x/D_0 \simeq 3{\cdot}5$ for the conical jet and $x/D_0 \simeq 4$ for the ellipsoidal jet.

The axial distribution of the peak turbulence intensity of the outer mixing region is shown in figure 9. Within the axial distance considered, $1 \leqslant x/D_0 \leqslant 7$, the peak turbulence intensity of the annular jet is slightly higher than those of the conical and ellipsoidal jets, while the results for the latter two jets are the same. The biggest difference is observed in the intermediate zone $2 < x/D_0 < 5$. This suggests that the effect of the subatmospheric pressure region on the peak turbulence intensity is mostly felt in this zone. In the fully merged zone the three jets have the same peak intensity.

The single-jet results of Laurence (1956) and Ko & Davies (1971) are also shown in figure 9. Within the initial merging zone comparison shows that the peak intensity of the single jet is slightly higher than those of the present three jets. In the intermediate zone, however, the single-jet results agree with those for the annular jet. In the fully merged zone the results for all the jets are the same.

	Initial merging zone, outer mixing region	Intermediate zone	Fully merged zone	Single jet
Non-dimensional axial distance	x/D_o	x/D_o	x/D_o	x/D_o
Non-dimensional radial distance	$(y-y_{0.5})/(y_{0.9}-y_{0.1})$	$(y-\frac{1}{2}D_e)/x$	$(y-\frac{1}{2}D_e)/x$	$(y-\frac{1}{2}D)/x$
Mean velocity ratio	$\overline{U}/\overline{U}_0$	$\overline{U}/\overline{U}_m$	$\overline{U}/\overline{U}_m$	$\overline{U}/\overline{U}_0$
Turbulence intensity	$\overline{(u^2)}^{\frac{1}{2}}/\overline{U}_0$ $(\overline{(u^2)}^{\frac{1}{2}}/\overline{U}_0)_{max}$	$\overline{(u^2)}^{\frac{1}{2}}/\overline{U}_0$	$\overline{(u^2)}^{\frac{1}{2}}/\overline{U}_0$	$\overline{(u^2)}^{\frac{1}{2}}/\overline{U}_0$

TABLE 1. Summary of non-dimensional parameters of annular jets.

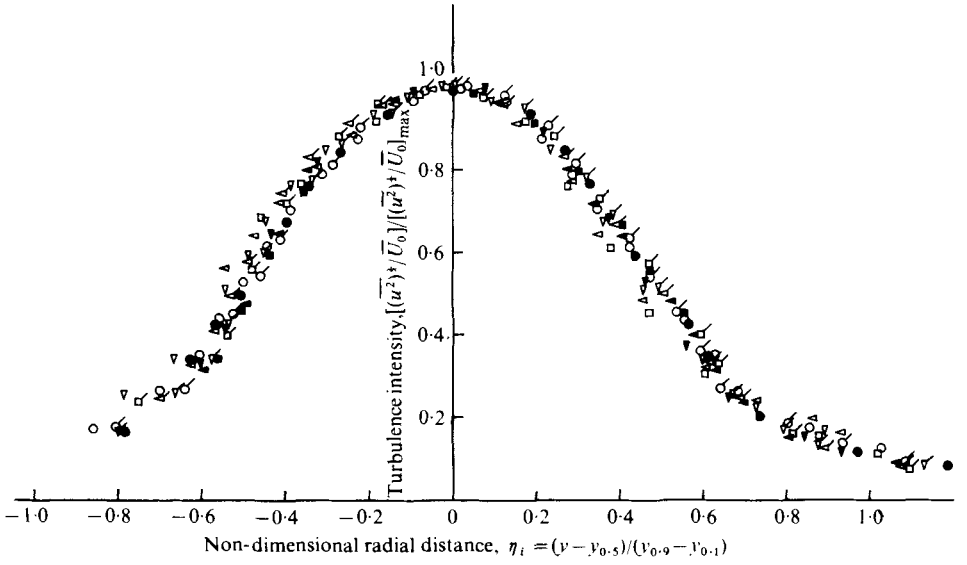

FIGURE 10. Similarity of turbulence intensity in initial merging zone. Symbols same as in figures 4 and 8.

Similarity

Similarity of the turbulence intensity profiles in different zones of the three jets is described in this subsection. The non-dimensional parameters which have been found for the similarity of the mean velocity profiles will be used to correlate with the local turbulence (table 1). The similarity curve for the initial merging zone of the three jets is shown in figure 10. The turbulence intensity ratio, i.e. the ratio of the local intensity to the maximum intensity in that particular plane, is correlated with the non-dimensional radial distance $\eta_i = (y-y_{0.5})/(y_{0.9}-y_{0.1})$. From this figure good similarity of the results within the initial merging region $y/D_o \leqslant 2$ is found for all three jets. Deviation starts to occur at $x/D_o \geqslant 3$.

Careful comparison of the results for the conical and ellipsoidal jets shows that their similarity curves are the same. When this curve is compared with that for the annular jet, the similarity curve of the latter tends to be displaced slightly towards

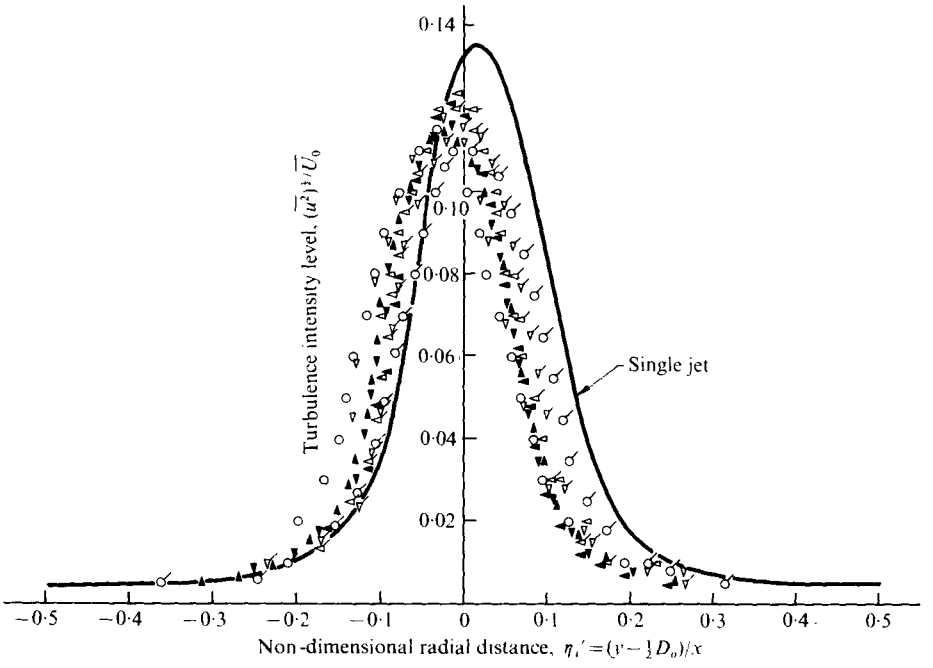

FIGURE 11. Similarity of turbulence intensity level in initial merging zone. Symbols same as in figures 4 and 8.

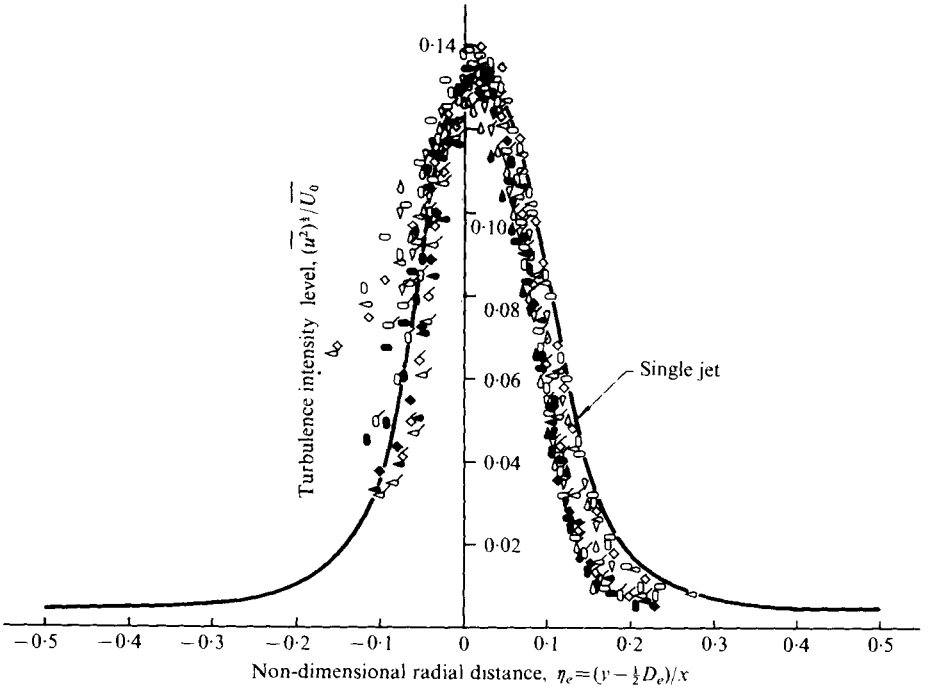

FIGURE 12. Similarity of turbulence intensity level in intermediate and fully merged zone. Annular: ⊂, $x/D_0 = 2{\cdot}5$. Conical: ●, $x/D_0 = 2{\cdot}5$. Ellipsoidal: ◁, $x/D_0 = 2{\cdot}5$. Other symbols same as in figure 6.

the central axis. This shift, though very slight, indicates the effect of the entrainment and the presence of the subatmospheric pressure region in the centre.

As has been shown by the mean velocity, the similarity of the turbulence intensity $\overline{(u^2)}^{\frac{1}{2}}/\overline{U}_0$ of the three jets with the non-dimensional radial distance $\eta_i' = (y - \frac{1}{2}D_o)/x$ is different from the single-jet results (figure 11). The peak of the intensity profiles of the three jets is found at $\eta_i' \simeq 0$ and is slightly more displaced towards the central axis than for the single jet. Among the three jets of this investigation the annular jet has the biggest displacement and the ellipsoidal jet the smallest of the three. This agrees with the results for the mean velocity shown in figure 5. However, the displacement of the turbulence intensity similarity curve is not as large as that of the mean velocity.

In the intermediate and fully merged zones $2{\cdot}5 \leqslant x/D_o \leqslant 7$, similarity of the turbulence intensity profiles has also been found (figure 12). Also as in the case of the mean velocity, the turbulence intensity $\overline{(u^2)}^{\frac{1}{2}}/\overline{U}_0$ correlates well with the equivalent non-dimensional radial distance η_e. For the annular jet, however, the similarity for $\eta_e < 0$ is not as good as that for $\eta_e > 0$. The reason may be the effect of the subatmospheric pressure region on the mixing. This poorer similarity for $\eta_e < 0$ is also found in the results for the conical and ellipsoidal jets, though to a lesser degree.

The similarity curves of the conical and ellipsoidal jets are basically the same. They are slightly different from and are slightly more displaced towards the central axis than that for the annular jet. The similarity curve for the annular jet is very nearly the the same as that for a single jet, while those for the other two jets are slightly different.

In the fully merged zone similarity of the turbulence intensity profiles with the non-dimensional distance y/y_c has been found not to be as good as that of the mean velocity. Thus the results are not included in this paper.

Results for an exit velocity of 30 ms^{-1} are also found to agree very well with the results presented above. Thus they are excluded from the present investigation.

5. Discussion

The mean velocity and turbulence intensity measurements made in the outer mixing region within the initial region of the three annular jets permit the isolation of three separate zones: the initial merging, the intermediate and the fully merged zone. Irrespective of the type of jet, i.e. annular, conical or ellipsoidal, the initial merging zone is found within the first two outside diameters downstream of the nozzle exit. It is within this zone that the annular potential core exists. The intermediate zone, where the mixing of the high velocity flow inherited from the potential core occurs, is found within the next three outside diameters downstream. After the intermediate zone there is the fully merged zone, where the flow has become fully merged and behaves like a combined jet.

In all three of these zones similarity of both the mean velocity and the turbulence intensity profiles in the outer mixing region has been found. In each zone, the same non-dimensional radial distance is found for both the mean velocity and the turbulence intensity. The similarity observed in the different zones further supports their division.

The difference in the entrainment in the centre of the jet in the three configurations is responsible for the difference in the displacement of both the mean velocity and the turbulence intensity profiles towards the central axis. This difference is more obvious in the initial merging zone, where the effect of entrainment is more obvious. In the intermediate zone a much smaller displacement is found. In the fully merged zone no difference is observed.

Very good agreement between the similarity curves for the present three jets and for a single jet is found. The initial merging zone corresponds to the initial region of the single jet where the potential core and mixing region are found. The intermediate zone corresponds to the transition region and the fully merged zone to the fully developed region.

REFERENCES

ABRAMOVICH, N. 1963 *The Theory of Turbulent Jets.* M.I.T. Press.

AYUKAWA, K. & SHAKOUCHI, T. 1976 Analysis of a jet attaching to an offset parallel plate. *Bull. Japan Soc. Mech. Engrs* **19**, 395–401.

CHIGIER, N. A. & BEER, J. M. 1964 The flow region near the nozzle in double concentric jets. *Trans. A.S.M.E., J. Basic Engng* **86**, 794–804.

DAVIES, P. O. A. L. & DAVIS, M. R. 1966 Hot-wire anemometer. *Inst. Sound Vib. Res., Univ. Southampton Rep.* no. 155.

DAVIES, P. O. A. L., FISHER, M. J. & BARRATT, M. J. 1963 The characteristics of the turbulence in the mixing region of a round jet. *J. Fluid Mech.* **15**, 337–367.

ELDRED, K. M. *et al.* 1971 Far-field noise generation by coaxial flow jet exhaust. 1. Detailed discussion. *Wyle Lab. Rep.* no. FAA-RD-71- 101, p. 1.

KO, N. W. M. & DAVIES, P. O. A. L. 1971 The near field within the potential cone of subsonic cold jets. *J. Fluid Mech.* **50**, 49–78.

KO, N. W. M. & KWAN, A. S. H. 1976 The initial region of subsonic coaxial jets. *J. Fluid Mech.* **73**, 305–332.

LAURENCE, J. C. 1956 Intensity, scale and spectra of turbulence in the mixing region of a free subsonic jet. *N.A.C.A. Rep.* no. 1292.

MILLER, D. & COMINGS, E. W. 1960 Force-momentum fields in a dual-jet flow. *J. Fluid Mech.* **7**, 237–256.

MOLLO-CHRISTENSEN, E., KOLPIN, M. A. & MARTUCCELLI, J. R. 1964 Experiments on jet flows and jet noise for field spectra and directivity patterns. *J. Fluid Mech.* **18**, 285–301.